Ting : A device to alert homeowners of scintillations which precede electrical fires

Stan Heckman, Christopher Sloop, Vyto Babrauskas, Eric Hoppmann, Oren Schetrit

October 2018

Table of Contents

Introduction and Background

Electrical malfunctions are one of the leading causes of residential home fires. Because of the hidden nature of the ignition source, electrical fires are a disproportionate cause of death [1]. Electrical fires are estimated to cause 420 deaths, 1,370 injuries, and $1.4B in residential damages annually [3].

Arc faults (also called arcs) are high-power, continuous electric discharges between two or more conductors—typically occurring in residential buildings when the integrity of an electrical wire is compromised [24] (e.g., through damage, corrosion, age, or loose connections, among other causes). As a result of the compromised insulation, small, sporadic electrical discharges begin to occur and the insulating material that surrounds the wire is carbonized. If the electrical discharges continue over time, the insulation is increasingly eroded and the electrical discharges increase in intensity. Eventually, the electrical discharges may become continuous arc faults, resulting in large flow of current and large releases of energy (with correspondingly high temperatures). If the arcing wire is in close proximity to wood framing, insulation, or similar combustible materials, the high temperatures produced by the arcs are high enough to produce fire [21]. Often times, these fires begin in walls or other hidden cavities, and gain significant heat and headway before they are detected by home occupants or smoke detectors, leading to significant damage.

The current solution to address these fires is an Arc-Fault Circuit Interrupter (AFCI). AFCIs are special types of circuit breakers that utilize electronic technology to “sense” different arcing conditions and shut off power to the circuit if such conditions are detected. AFCIs are required in the National Electric Code (NEC) in new home construction and renovations. A major challenge with AFCIs is that they require a complete electrical system upgrade to install in existing homes, and are thus cost prohibitive, and challenging to deploy at scale. With installation, each AFCIs cost $160 to $260+ per breaker, so installed costs would run on average $2,000 per home [4]. In 2017, the AFCI market size was $3.7B [5]. It is important to note that AFCI’s theory of operation is similar to that of Ting, in that electrical signals from arc faults travel down branch circuit wiring to the main electrical panel, where electronics in the AFCI breaker detect such signals.

> Alternatively, companies such as CurrentSafe offer a network of electricians to manually inspect homes for electrical fire hazards, typically at a cost of $1,500 for a 1,500 square foot home. That amounts to $2,500 for an average sized home, and with the 12,000 visits per year they do, homeowners today are paying $30 million per year for electrical fire hazard detection.

To prevent dangerous and costly electrical fires, while providing a cost-effective and scalable solution, the Whisker Labs team has developed smart plug-like technology that will detect and alert homeowners to the presence of damaged and arcing wires. An accompanying smartphone application and team of experts will guide homeowners through the necessary steps to mitigate the fire risk. The following technical paper documents the physics and technology leveraged by the Whisker Labs Ting sensor.

Fire Precursor Physics

Electrical fires occur when a conductor fails to conduct or an insulator fails to insulate. [9] Conductors fail to conduct because of joint fractures, the last strand of a cable breaks, or an outlet or push in connection becomes loose, leaving conductors barely touching with too small a surface area of connection. The resultant heating of the conductor may exacerbate the problem by causing surfaces to oxidize and become even less conductive [10]. The resultant heating of nearby insulators may exacerbate the problem by releasing gases that chemically attack the remaining conductor [21].

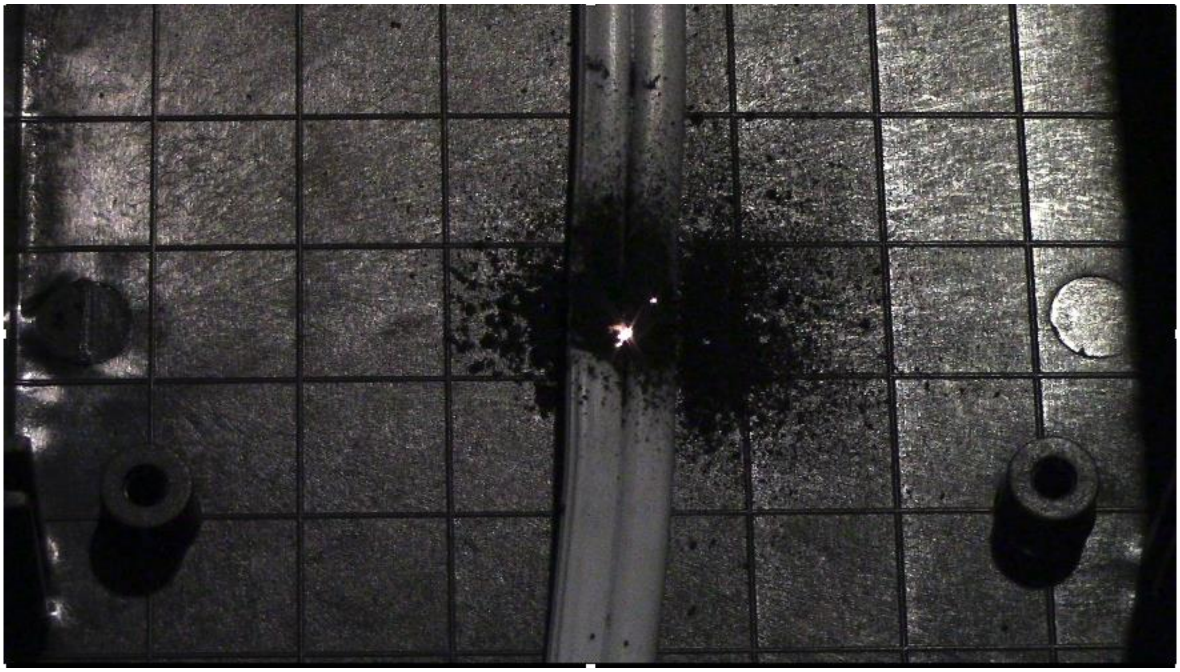

FIGURE 1 SCINTILLATION CARBONIZING INSULATION TEST WITH GRAPHITE POWDER

Insulators fail where a flexible cord or rigid insulator fractures, or where an intended opening in the insulation becomes covered with pollutants or water. Fractures may be caused by defects in manufacturing, hammer blows in construction, or repeated stress is use. Each time a tiny electrical failure occurs across one of these fractures, a bit more of the insulator is damaged, (usually) extinguishing the immediate failure, but (usually) making future failures easier. Most organic insulators "char", slowly turning into more conductive simpler organic materials through a process aptly named "carbonization of insulation" [7].

Arcing along a carbonized path produces "scintillations", dim flashes of red, orange, yellow, or white light. Scintillations and the fault currents associated with them are sporadic, highly intermittent. Arc tracking is a slow process which takes weeks, months or years [11]. Yearance [12] reports times to mature to fire ranging from hours to 40 years.

As scintillations and fault currents become more active, they generate pulses with high frequency content which propagates through the home’s electrical network. Subsequent sections of this white paper will document how traditional communication signals are transmitted over the electrical network—commonly referred to as power line carrier communications—and will explore the similarities between fire pulse signals and traditional power line carrier communication signals.

Home Electrical Infrastructure as a Communication Medium

The wires that provide power to appliances in buildings are the medium over which fire precursor signals travel from origin to sensor. Precursors are impulsive discharges and result in electromagnetic signals that travel along the power distribution wires in a building. Every location in the wiring (both fixed house wiring and mobile cords to devices and appliances) has a transfer function to every outlet in the house, and the precursor signals arrive at the sensor modified by this transfer function. The Whisker Labs technology leverages methods developed in power line carrier communication techniques to measure and identify very broad frequency content which travels through a home's electrical network similar to power line carrier communication.

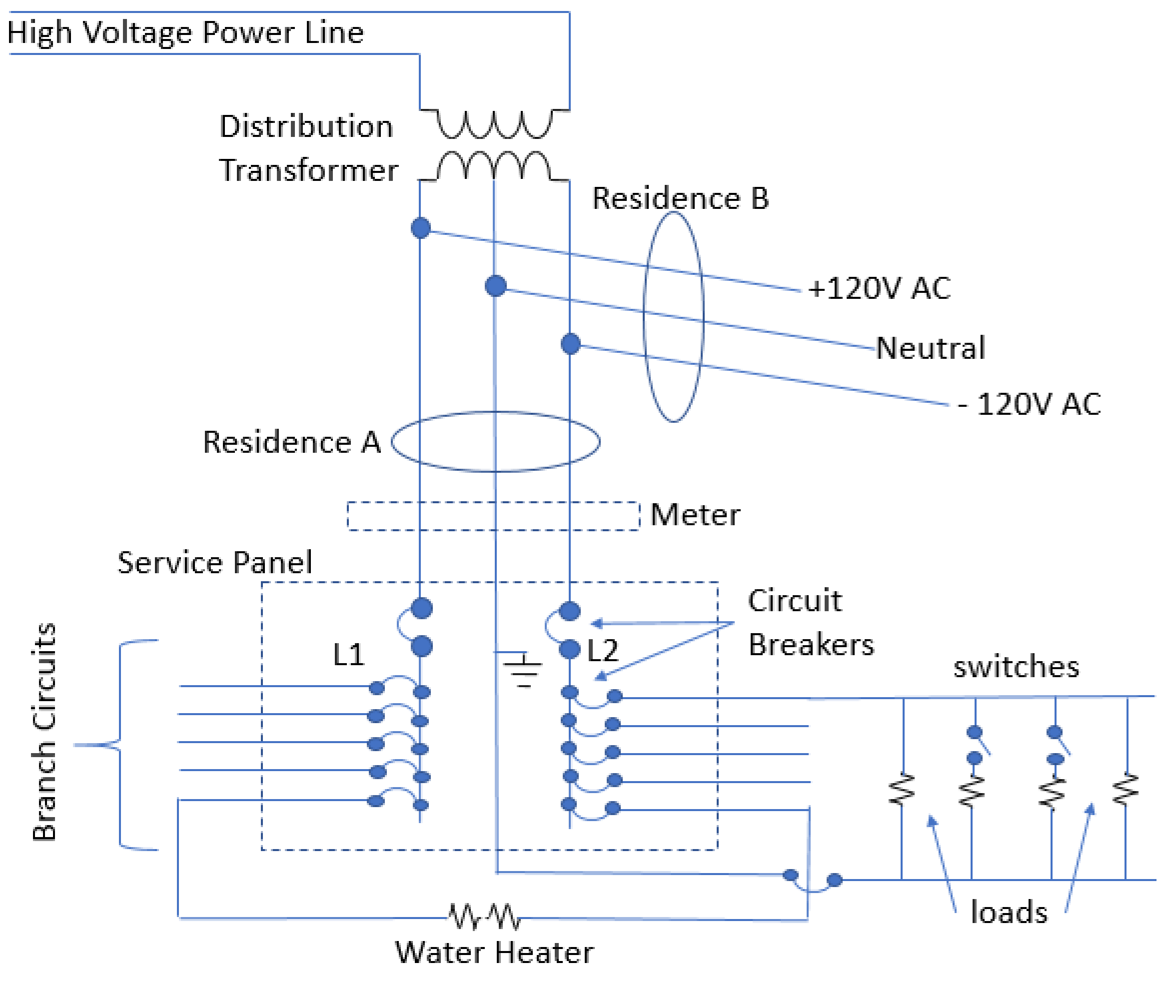

FIGURE 2 SINGE LINE DIAGRAM DEMONSTRATING RESIDENTIAL ELECTRICAL NETWORK; INCLUDING L1, L2, AND NEUTRAL. COMMUNICATION IS POSSIBLE FROM ANY CIRCUIT ON L1 TO ANY CIRCUIT ON L2. [20]

Communicating using power lines has been considered and used since the turn of the 20th century [11,12]. In the last twenty years, various companies have released products that provide 100Mbps to 1Gbps local area network communication over in-building electrical distribution systems. This work resulted in the standardization of power line communication in IEEE 1901 [15] and the widespread availability of “ethernet over powerline” adapters for consumer use [16], and broadband communication over in-building power lines is a mature technology.

There are two major issues associated with communicating over power lines (i.e., the channel): the transmission and attenuation characteristics of a transmitter and receiver on different circuits of the building and the channel noise environment. The research literature is mature in both areas with peaks in publication in 2008. The powerline channel is challenging because there are many discontinuities due to branches (e.g., each outlet on a circuit) as well as loads with frequency and time dependent impedances (e.g., due to different device power draw, construction, and on vs off characteristics). The devices that are responsible for the time variance are also responsible for both narrow and broad band noise injection due to switching power supplies and other non-linear equipment elements. A good overview of the state-of-the-art in powerline communication can be found in [17].

The power line channel transmission characteristics have been the subject of significant field measurement and modeling activities that culminated in the IEEE 1901 standard ratification in 2010 [15]. Figure 3 shows field-collected measurements of the communication channel for indoor, residential power-line networks. The top represents multiple pairs of transmitters and receivers on the same circuit. The bottom chart shows multiple transmitter and receiver pairs where the units are on different circuits [18]. Measurement results taken in Spain show similar characteristics confirming that changes in mains configuration and wiring style result in similar overall characteristics [17]. The more interesting and difficult case is the second (lower) chart in Figure 4 shows the transfer characteristics for three different circuits and a comparison 20m long cable measured in a lab setting [20].

These charts show variable frequency dependence for a particular channel but relatively flat attenuation on average. The sites used for gathering these data were varied in size from apartments to large homes and in age of construction. The channel characteristics are similar in many ways to stationary wireless communication channels. Wireless channels experience fading (i.e., frequency, position, and time dependent attenuation) due reflections of signals off objects in the environment (i.e., multipath induced fading). The same effect is at play here because discontinuities, mismatched impedances, and branches in the wiring result in signal reflections. In the time domain, these reflections manifest themselves as amplitude and time shifted copies of the original signal arriving at the receiver. In the frequency domain, the frequency components of these copies either constructively or destructively interfere causing peaks and notches in the transfer characteristic as observed in the charts.

Power line communication systems use the same techniques for signal encoding and noise resilience that are employed in broadband, wireless local area networks (e.g., IEEE 802.11n), chiefly orthogonal frequency division multiplexing (OFDM). OFDM is a good solution because it is a technique for spreading information across a wide band of the spectrum while also reducing the impact of signal dispersion and fading.

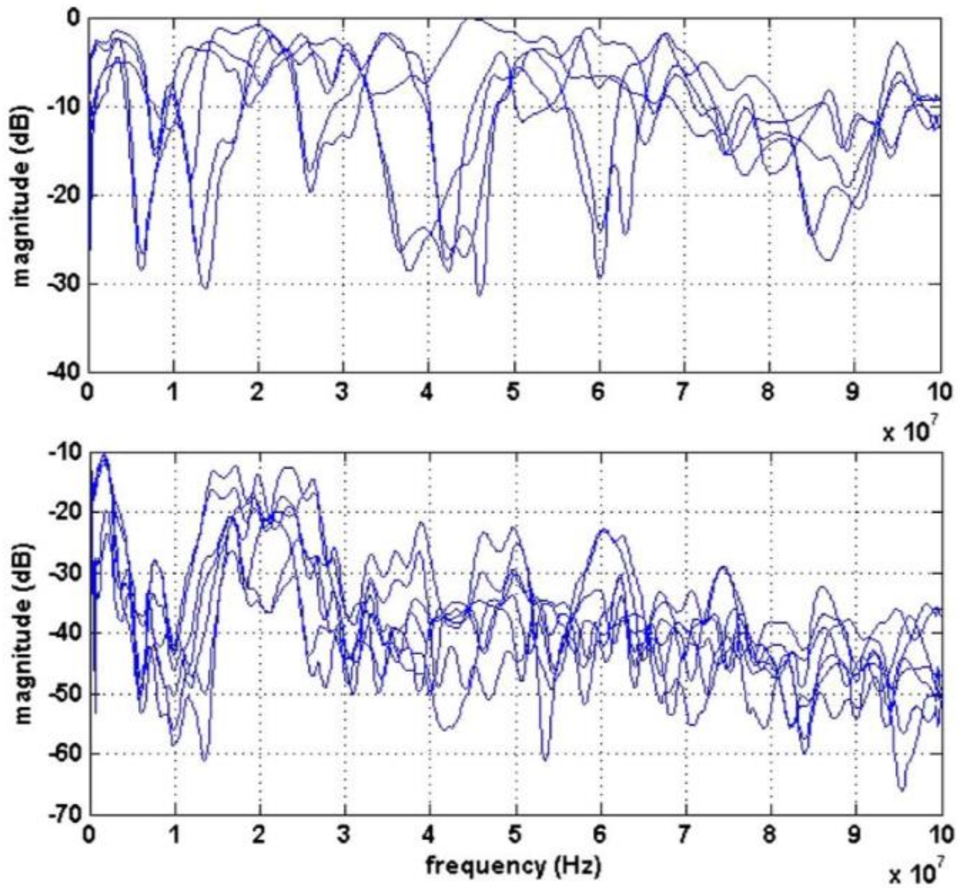

FIGURE 3 CHANNEL ATTENUATION FOR TRANSMITTER/RECEIVER PAIRS ON THE SAME CIRCUIT (TOP) AND DIFFERENT CIRCUITS (BOTTOM) IN US RESIDENTIAL HOMES [18].

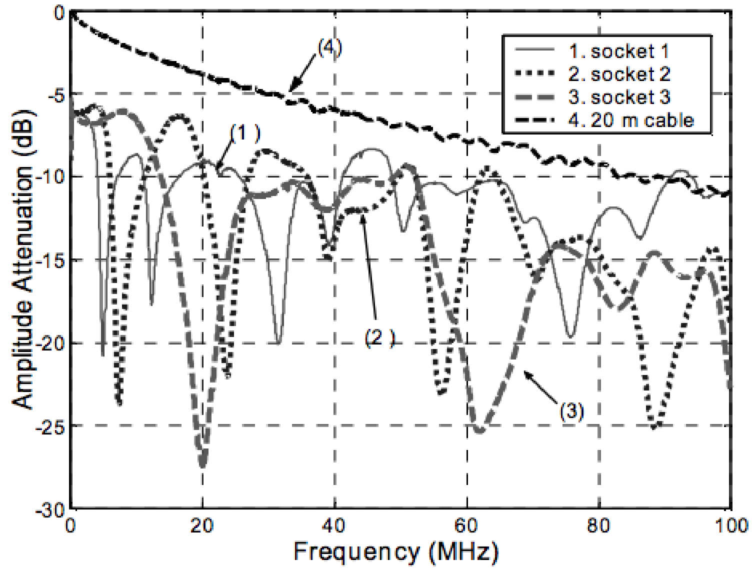

FIGURE 4 CHANNEL ATTENUATION FOR DIFFERENT RECEIVER LOCATIONS IN A HOME COMPARED TO A LABORATORY SETUP WITH UNINTERRUPTED POWER CABLE [20]

The power line environment is challenging for communication, but market success of Ethernet over power line products demonstrate that it is possible for broadband signals to traverse the complicated electrical network. Narrow band communication is very challenging due to extreme frequency selectivity that is dependent on individual, time varying channel conditions. Circuit to circuit signal attenuations are significant but are typically less than 50dB making it possible for signals sourced almost anywhere in the electrical wiring to be detected at a receiver elsewhere in the house wiring (i.e. at an electrical socket).

Fire Precursor Signal Characteristics

The arcing along carbonized or damaged conductors causes "scintillations". These draw current in a variable pulse-like fashion. These current pulses have typical durations of several microseconds. Durations range from less than one microsecond to tens of microseconds. Typical amplitudes are tens of milliamps. The largest pulses draw more than 100 milliamps. Current pulses correspond to dim yet visible flashes of red, orange, yellow, or white light. In addition to the visible component, the pulses also emit infrared and radio frequency (RF) energy.

To test and evaluate signal characteristics, we developed techniques for capturing the current component of the above described scintillation pulses. Figure 5 shows a diagram of a test fixture used for capturing fire precursor pulses. The test fixture includes a power cord (A) plugged into a standard wall outlet with Hot, Neutral and Ground conductors. The power cord is spliced to include resistors (labeled R1, R2, R3) through which any currents creating by scintillations or electrical discharges must pass. The end of the power cord is connected to a plug through which various test apparatuses can be connected. In the case of this diagram, we have connected an apparatus which is a plastic NEMA enclosure through which a damaged extension cord is passed. The damaged electrical cord can be exposed to various substances which cause electrical discharges to occur. For example, the substance could be graphite powder, water or a solution of water, soap and salt. A differential analog to digital converter measures the voltage across a resistor of known resistance to calculate the current flow through the resistor. Resistors of various sizes are selected to provide appropriate amount of gain depending on the expected peak current generated by exposing the damaged cord to various substances.

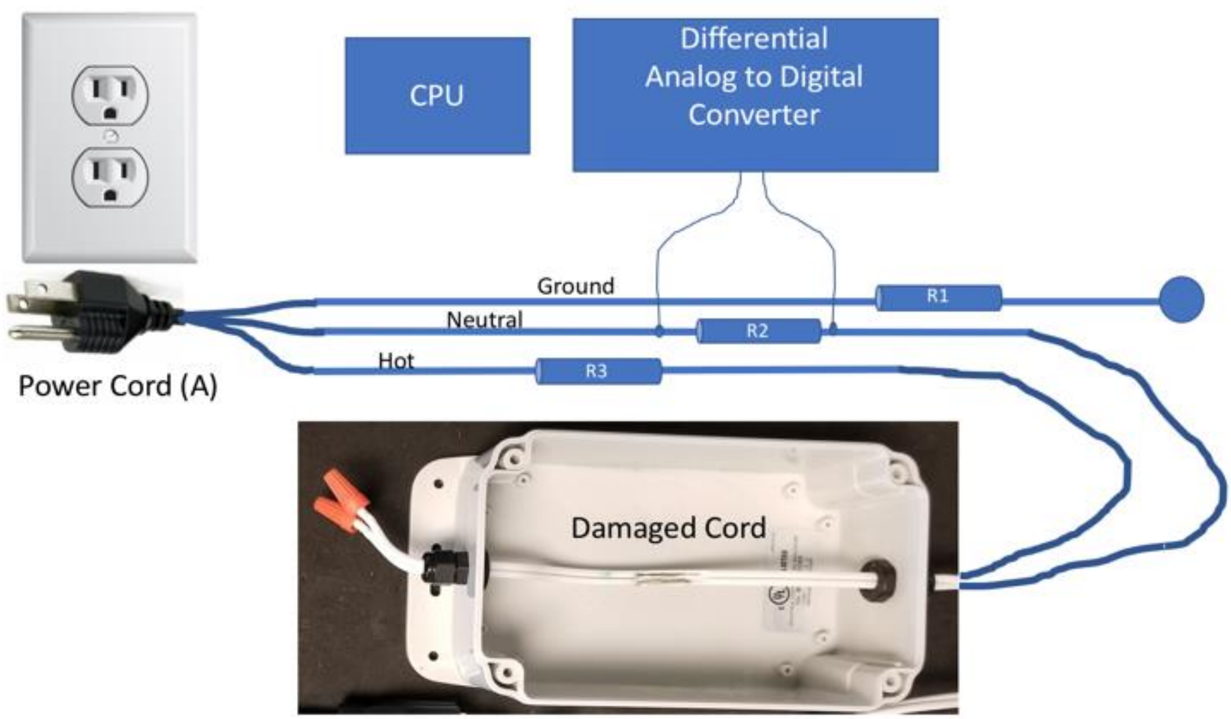

FIGURE 5 DIAGRAMMATIC REPRESENTATION OF A TEST FIXTURE USED FOR CAPTURING FIRE PRECURSOR PULSES

In the following chart one can observe the current drawn by an arc pulse. This individual pulse is taken from a longer time series showing many pulses over a period of time as shown below. The pulses come in groups of many pulses packed together in groups with relative periods of quiet between groups. Insulation is damaged ("carbonized") by tiny electrical discharges.

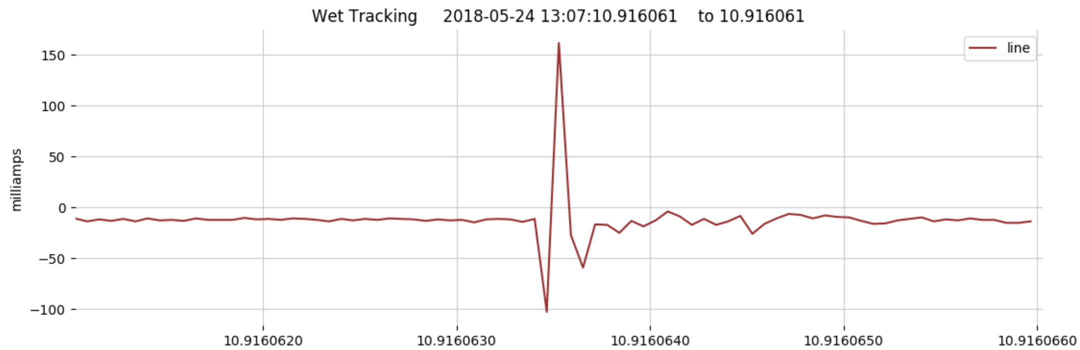

FIGURE 6 TIME SERIES PLOT OF CURRENT DRAWN BY MICRO-PULSES

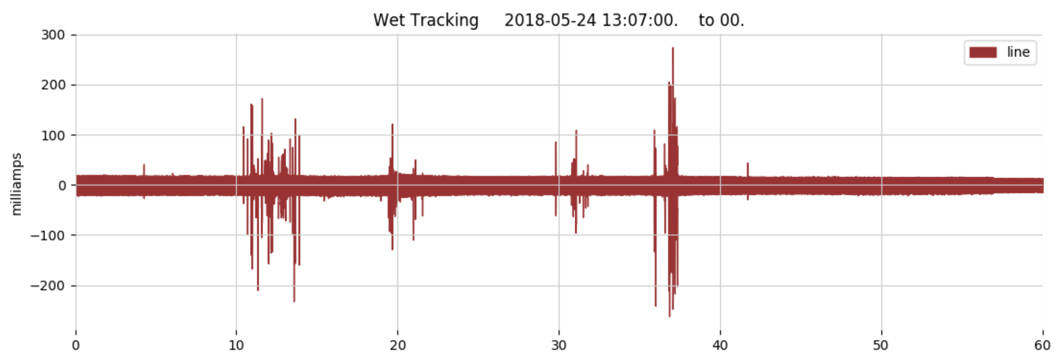

FIGURE 7 TIME SERIES PLOT OF CURRENT DRAWN BY MICRO-PULSES

The arc precursor pulses contain very broad frequency content which travels through a home's electrical network similar to power line carrier communication. The rapid start of current and the rapid stop of current radiate UHF and VHF. The tens or hundreds of nanoseconds duration radiates HF. Because the current in one pulse is generally one polarity, pulses also radiate at all frequencies lower than HF.

Figures 8, 9, 10, 11, 12 show example fire pulses captured in the laboratory. The top of each chart shows the time series data captured and the bottoms shows a spectrogram of the same data. In the spectrogram, the frequency bins of the time-resolved FFT are on the y-axis with the time of the x-axis (matching the time axis of the time domain top plot).

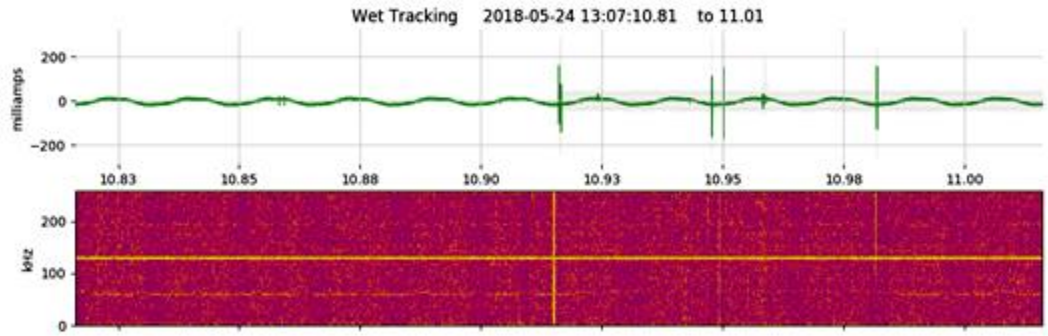

Figure 8 Example time series and spectrogram plot of laboratory measured fire precursor (scintillation) pulses showing broad frequency content in the range of 0 - 300 kHz. The last pulse has less low frequency than high frequency energy (a high-pass or blue characteristic).

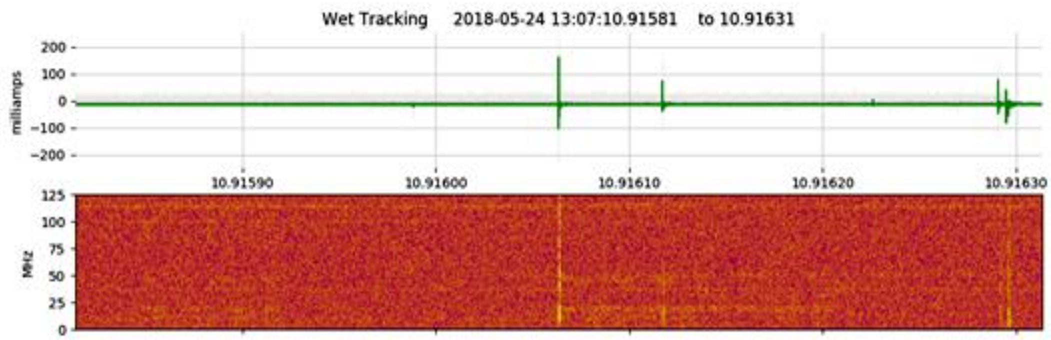

FIGURE 9 EXAMPLE TIME SERIES AND SPECTROGRAM PLOT OF LABORATORY MEASURED FIRE PRECURSOR (SCINTILLATION) PULSES SHOWING BROAD FREQUENCY CONTENT IN THE RANGE OF 0 - 125 MHZ. THE LAST PULSE HAS A LOW-PASS OR PINK CHARACTERISTIC WITH MUCH OF THE ENERGY BELOW 25 MHZ.

FIGURE 10 EXAMPLE TIME SERIES AND SPECTROGRAM PLOT OF A LABORATORY MEASURED FIRE PRECURSOR (SCINTILLATION) PULSE SHOWING BROAD FREQUENCY CONTENT IN THE RANGE OF 0 - 125 MHZ. THIS PULSE HAS A SLIGHTLY LOW-PASS OR PINK CHARACTERISTIC WITH SIGNIFICANT ENERGY ACROSS THE SPECTRUM BUT WITH SOME GAPS.

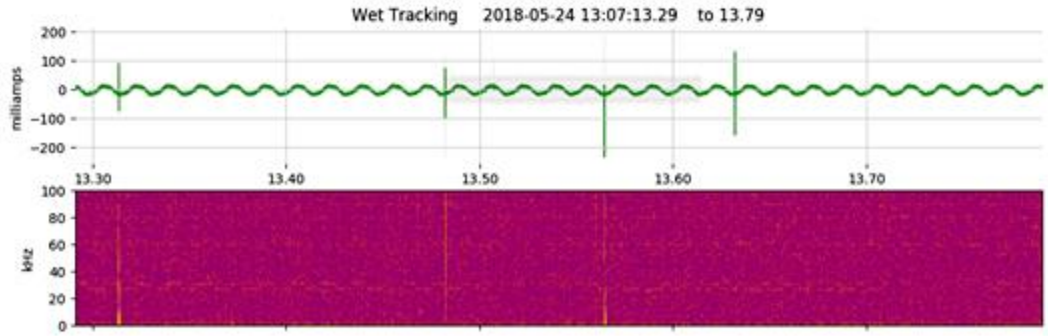

Figure 11 Example time series and spectrogram plot of a laboratory measured fire precursor (scintillation) pulse showing broad frequency content in the range of 0 - 100 kHz. These pulses show energy across the spectrum. The pulses are slightly colored with different characteristics but are all notably broadband.

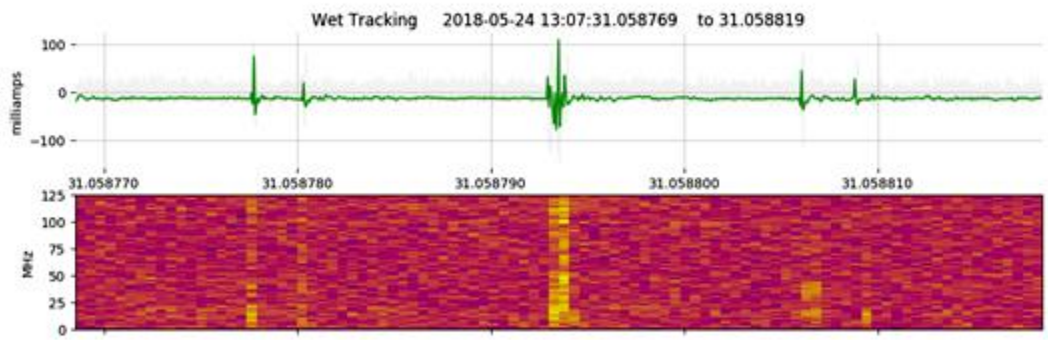

Figure 12 Example time series and spectrogram plot of a laboratory measured fire precursor (scintillation) pulse showing broad frequency content in the range of 0 - 125 MHz. Most pulses show energy across the spectrum.

These figures show different pulses and different frequency regions of interest. The common characteristic across all pulses is that the pulses are broad in frequency hence narrow in time. All pulses have significant content in the range of 10 kHz to 10 MHz. The pulses also have significant energy content up through 100 MHz and beyond, as expected given the narrow pulse duration.

Detecting Fire Precursor Signals

The broadband characteristics of the pulses (Figures 8-12) are convolved with the electrical infrastructure transfer function (Figure 3, Figure 4) before they are received by the receiver. The Ting sensor receiver consists of custom-built hardware and digital signal processing capable of digitizing, detecting, and interpreting the medium to high frequency content contained in the pulses. The overall system design takes into consideration the signal characteristics, the channel transfer characteristics, and the noise environment.

The precursor pulses are broadband and grouped together into clusters of pulses. The broadband nature means that as long as the channel passes a sufficient fraction of the bandwidth of the signal, some of the signal will pass through the channel. The clustered nature of the pulses mean that many pulses occur over relatively short periods of time. It is not necessary to observe all pulses, and observation of a fraction of the pulses is sufficient for detection. The short duration of the pulses means that the signal energy is concentrated in a short time period. Because power is energy per unit time, the pulses have high instantaneous power. The pulses are not locked in phase to the AC signal and occur at random times within the AC cycle. (Because it requires a voltage potential difference, we are more likely to see large pulses at the peaks of the voltage cycle and smaller pulses as we approach the zero crossings)

The channel passes energy across a wide frequency spectrum, but the channel is marked with a large number of reflections. This results in notches and peaks in the transfer characteristic. The literature shows that channels tend to pass energy in the 0 - 15 MHz range but do not do so uniformly with respect to frequency.

The literature discusses a variety of noise sources that are either nearly constant, cycle synchronized impulsive, or asynchronous impulsive. From the high instantaneous power of the signal, the random distribution of the pulses in the cycle, and the high pulse density during fire precursor activity, it follows that most fire pulses should be detectable across the home electrical infrastructure in virtually every pulse activity period.

Developing Testable Fire Signals

Since the Ting sensor is designed to be a single device plugged into a single outlet anywhere in the home, we set out to demonstrate the effectiveness of the device in detecting fire precursor pulses that occur at any location within the home.

One possible way to accomplish this would be to take a damaged cord that is producing fire precursor pulses to many homes and measure how well pulse signals are detected from other outlets in the home. The drawback of this approach is that it would take a significant amount of time to send a trained technician that can safely produce the signals and the study would only measure the signals over a short period of time—while someone was monitoring the system within the home. No reasonable individual would welcome a damaged (and hazardous) electrical cord in their house for an extended period of time.

The alternate and more scalable approach we have taken is to develop a “Proxy” device which can replay fire signals that are produced and recorded in the laboratory by real fire precursors. This proxy device allows for economical deployment of hundreds of units to varying types of homes across the country, along with an ability to track signal detection performance over long periods of time.

The Proxy device utilizes a digital to analog signal converter and power amplifier coupled to the electrical system via a power capacitor to simulate the fire precursor signals. The digital to analog converter can produce signals at 120 MHz for short periods of time. The CPU is phase locked with the zero crossing from the power mains to generate pulses that occur at appropriate locations in the phase. Pulse information is read by the CPU from the flash memory and recorded pulses are reproduced through the D/A converter and Power Amplifier. A block diagram of the Proxy device can be seen in in figure 13.

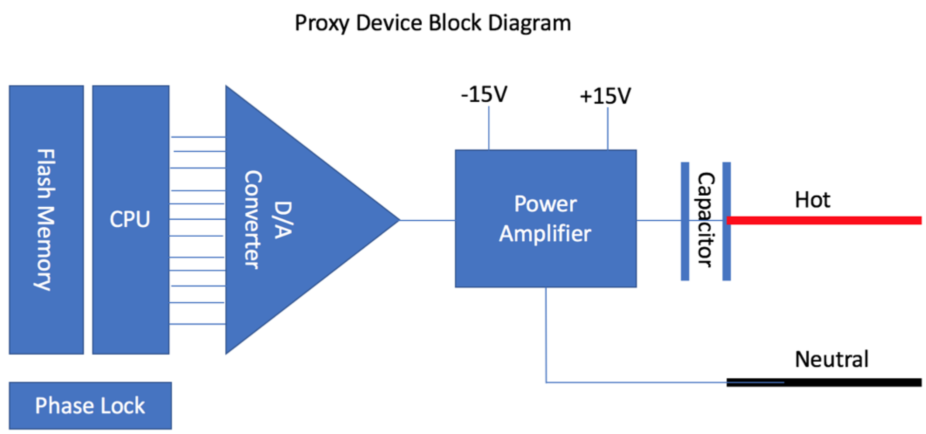

FIGURE 13 - BLOCK DIAGRAM OF PROXY DEVICE USED TO SIMULATE FIRE PRECURSOR PULSES ON THE POWER LINE.

The Proxy device, when deployed in many homes helps answer to the following questions:

1) How well do the fire precursor arcing signals travel in the home electrical system?

2) How well do our algorithms do at identifying electrical fire signals and distinguish these signals from those created by other appliances in the home?

To determine how well fire precursor pulse signals travel in the home electrical system, we deployed the test fixture as seen in Figure 5 to a test home. The test home is a large single-family home of approximately 4,000 square feet. The home has typical types of electronics equipment including flat screen televisions, audio equipment and computers. The electronics equipment is typically protected by surge suppressor power strips.

Figure 14 shows data collected from a test home. The graph in (a) shows 60 seconds of a measurement of peak analog to digital converter output from two sensors. The sensor labeled “Same Ting” (blue) is on the same 120V leg/phase, and is on the same branch circuit as the test fixture. The sensor labeled “Other Ting” (red) is on the opposite 120V leg/phase of the power network on a different branch circuit. Larger amplitude signals indicate times when the test fixture is creating fire precursor pulses. For example, in graph (a) we see the blue line and red line jump up to approximately 2400 raw digital units in the area highlighted in yellow indicating that both sensors detected a fire precursor pulse.

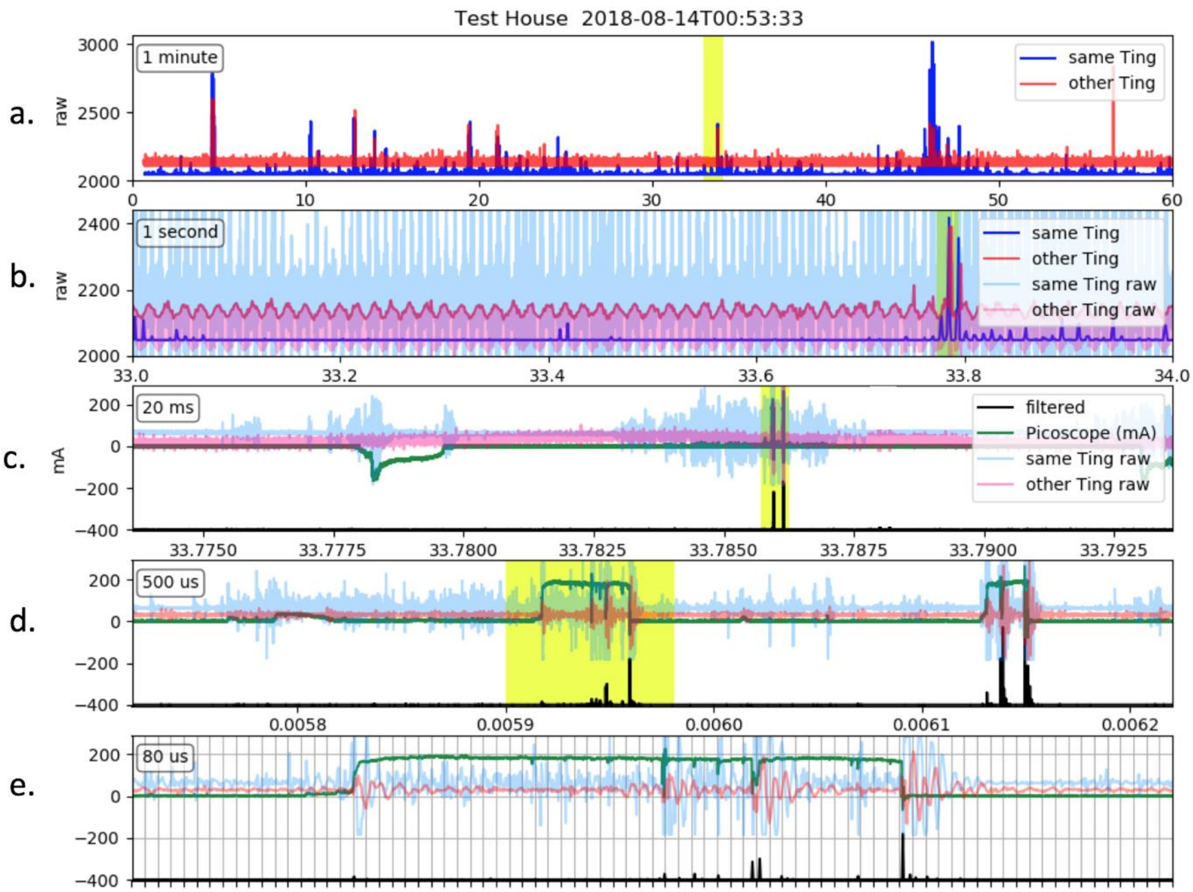

FIGURE 14 – GRAPHS SHOWING DATA GATHERED FROM A TEST HOME WHERE SCINTILLATIONS WERE CREATED.

The graph labeled (b) if figure 14 shows the highlighted period from graph (a) zoomed into one second of time. In the graph labeled (c) we further zoom in to 20 milliseconds of time which is denoted by the yellow highlighted area in graph (b). In graph (c), we show the measurement of current (green) through a 10-ohm resistor on the hot line of the test fixture (see R3 in figure 5). This is the current that flows when breakdown on the insulator occurs and is observed as an electrical discharge and is evidenced in the form of heat and light. Graph (d) and (e) show further zoomed in periods of the current flow through the 10-ohm resistor and the resultant waveforms as seen by the Ting sensors.

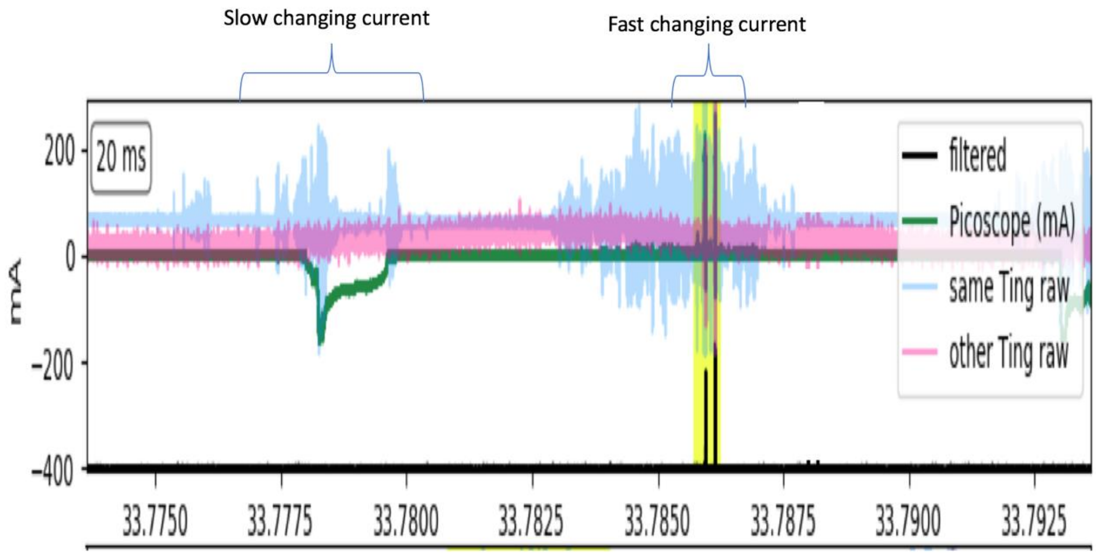

FIGURE 15 – TRANSMISSION EFFICIENCY OF ELECTRICAL DISCHARGE CURRENT PULSES.

Figure 15 shows a more detailed version of figure 14(c) which highlights two times where electrical breakdown occurred and which we measured current through our 10-ohm resistor. What we see in this example is that electrical breakdown can produce currents that change slowly over a time period of many microseconds, to currents that start and stop very fast, on the order of nanoseconds to tens of nanoseconds. As can be seen in figure 15, the slowly changing currents produce a visible signal in the sensor on the same circuit ("Same Ting"), but not in the sensor on a different leg ("Other Ting"), while the fast-changing currents are visible in the signals from both Ting sensors.

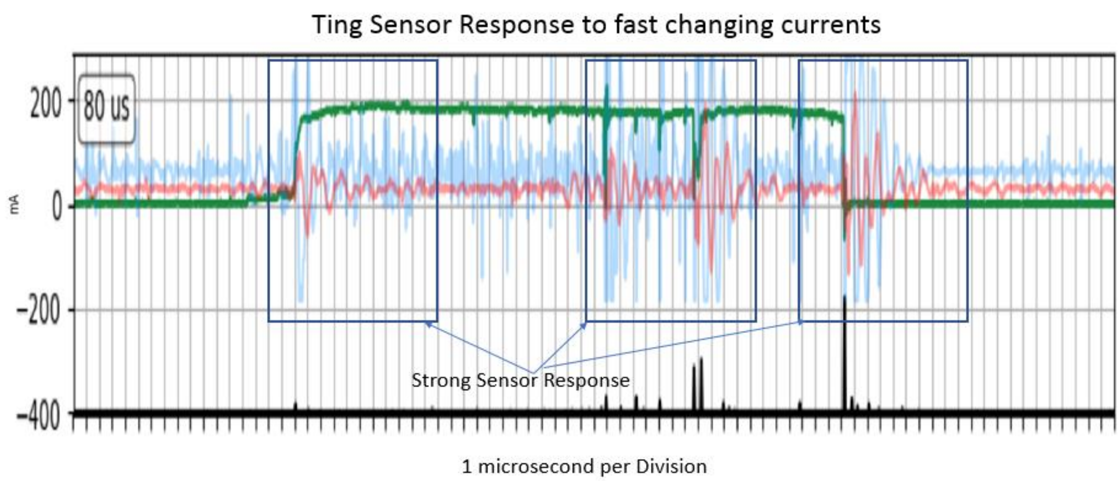

FIGURE 16 – THE TING SENSOR HAS A STRONG RESPONSE TO FAST CHANGING CURRENTS CREATED BY SCINTILLATIONS ON ELECTRICAL WIRING.

Figure 16 shows a more detailed look at one of the individual pulses from an electrical discharge with some information on the current change rates as the current starts flowing, then experiences several interruptions to the current flow until finally being extinguished. Note that at each fast change in the current, both Ting sensors see a sharp rise in signal followed by a characteristic ring-down. This demonstrates that the characteristic of the electrical discharge that makes the biggest impact on how well signals travel through the electrical network is the very fast rise time and fall time of the currents. Note that as the discharge starts, we see the characteristic ring down signal, but as the current continues at the same level, the sensor on the opposite phase does not have a strong response. This is an important finding for the development of our Proxy device as it means that as long as our Proxy device can simulate the fire precursor fast pulse currents rise and fall times, then we are re-creating the most relevant part of the signal and don't need to re-create the longer continuing currents.

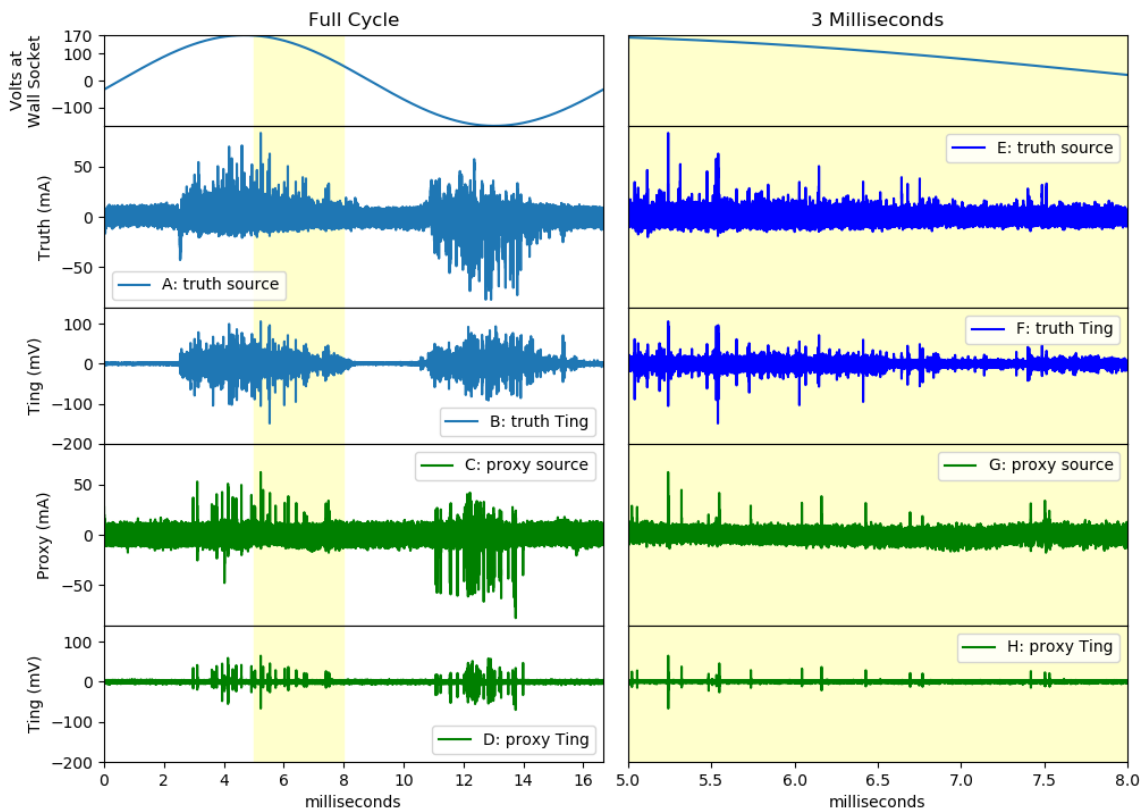

FIGURE 17 – DETAILED COMPARISON OF ACTUAL FIRE PRECURSOR PULSE CURRENTS AND A PULSES CREATED BY THE PROXY DEVICE. IN THE LABORATORY WE DAMAGED INSULATION BETWEEN CONDUCTORS UNTIL CARBONIZATION OCCURRED, THEN WE MEASURED THE CURRENT DRAWN BY THE SCINTILLATIONS (A). THE HIGH FREQUENCY PARTS OF THAT CURRENT TRAVELED THROUGH THE ELECTRICAL BOX ONTO A DIFFERENT CIRCUIT WHERE THE TING WAS PLUGGED IN, PRODUCING A VOLTAGE WE MEASURED AT THE TING (B). WE PROGRAMMED OUR PROXY TO REPRODUCE (ONLY THE LARGEST PULSES OF) CURRENT (A). THE PROXY PRODUCED CURRENT (C) ON ITS OWN CIRCUIT. THE HIGH FREQUENCY PARTS OF THIS CURRENT TRAVELED THROUGH

THE ELECTRIC BOX AND PRODUCED VOLTAGE (D) AT THE TING. PLOTS E,F,G, AND H ZOOM INTO PLOTS A,B,C, AND D.

The Proxy, which functions as our arbitrary waveform generator, reproduces laboratory waveforms imperfectly. It can only generate voltage steps at certain digital clock edges and it can only generate steps of certain discrete amplitudes. We perform lossy compression on the data, preserving only the largest peaks and preserving their shapes. The impedance of our proxy is not the same as the impedance of a damaged portion of insulator, so reflections from our proxy differ from reflections from a damaged cable. So, we need to check that our proxy is sufficient to produce signals at the Ting similar to the signals produced by real scintillations in damaged insulation.

We tested this by damaging insulation in the laboratory, measuring the currents produced by scintillations in the damaged insulation, and simultaneously measuring voltages produced by those scintillations at a Ting on a different circuit in our laboratory. We then programmed our proxy to replay the scintillations we measured, replaced the damaged insulation with the Proxy, and again simultaneously measured currents produced at the proxy and voltages produced at a Ting on a different circuit.

Figure 17 shows the results. 17A shows the current we initially measured in the laboratory from damaged insulation. 17B shows the voltage a Ting measured at another circuit, produced by the current pulses shown in 17A. 17C shows the current produced by our proxy, and 17D shows the voltage measured by a Ting on another circuit. Figures 17E through 17H show the same at a higher time resolution. The Ting voltages produced by the proxy are not identical to those we initially measured, but they are similar enough to use.

A second characteristic of fire precursor pulse signals that determine if they travel through the house is the amplitude of the pulse. Larger amplitude pulses produce a larger response in the Ting sensor. The relationship between the amplitude of the current and the size of the Ting sensor response can be seen in graphs 17E and 17F. Larger current amplitudes in 17E are observed as larger sensor responses in 17F. Similarly, larger amplitude currents produced by the proxy, result in larger responses at the Ting sensor (see graphs 17G and 17H). Currents on the order of 25mA are sufficient to produce a response in the Ting sensor with sufficient signal to noise ratio to be detected.

Fire precursors can generate thousands of pulses over a single power cycle a large percentage of which are not large enough in amplitude to travel through the electrical infrastructure and be seen by a Ting sensor on the opposite leg. The Proxy device is capable of producing a limited number of pulses per cycle. The device is programmed to focus on generating the largest and fastest pulses which are expected to be detected throughout the house. The Proxy device communicates with a server to notify the server of times which it is operating and which mode it is operating. In this case, it is very easy to correlate the times where the Proxy indicates it is running to Ting sensor output to verify that the sensor detects the signal. In the case of this white paper, the proxy was programmed to create fast pulses with amplitudes that ranged from 0 milliamps to 300 milliamps. Figure 18 shows a histogram of the amplitude of pulses found in a five second set of data that was acquired in the lab, labeled “truth” (blue). Additionally, a histogram of the amplitude of pulses re-created by the proxy is shown in orange. Generally, the counts of proxy pulses is less than from our truth data source. As described above, this is because of the limits of the proxy device memory to hold enough data to reproduce every pulse, so we focus on reproducing the largest pulses.

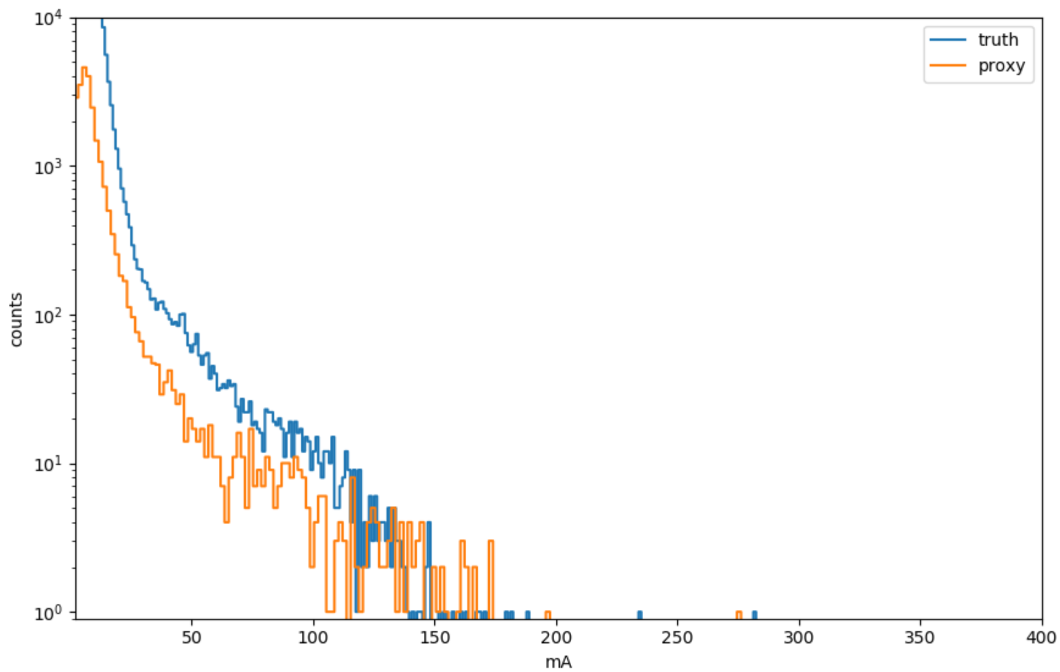

FIGURE 18 – HISTOGRAM OF PEAK CURRENTS FROM TRUTH FIRE PRECURSOR SIGNALS SHOWN IN BLUE. HISTOGRAM OF THE PEAK CURRENTS REPRODUCED BY THE PROXY SHOWN IN ORANGE.

Note that pulse current amplitudes in our proxy test data set are small in comparison to the peak amperes which trigger arc fault circuit interrupters. An AFCI will trip at about 50 amps for a parallel arc and 5 amps for a series arc [26]. By detecting pulse currents with these small amplitudes, we are able to alert a homeowner well in advance of the level at which the arcing becomes dangerous and fire hazard is imminent. This timeframe between when scintillations are detected and the arc grows large enough to be dangerous can be on the order of hours to years [11].

Having demonstrated that fire precursors create signals on the power network that travel throughout and can be detected by a single Ting sensor, the second question for detection efficiency relates to how well we can distinguish between fire precursor signals and man-made or other interfering signals which can be sensed on a power line. Fire precursor signals exhibit characteristics which are exploited for identification.

1) The fire precursor pulse signals are on average larger near voltage peaks and weakest, approaching zero near the voltage zero crossings.
2) Pulse signals are randomly distributed in time across multiple cycles and are randomly distributed across the phase.

Figure 19 shows a “color plot” of how fire precursor signals look over time. Time on the color plot is increasing from top to bottom. Each row of the color plot is representative of a single power cycle with the rising half cycle indicated on the left and the falling half cycle indicated on the right. The color scale indicates the amplitude of HF signals detected at various places in the power cycle phase. For parallel arcs, the HF amplitude increases at the peaks of the power cycle and goes to zero at the zero voltage crossings.

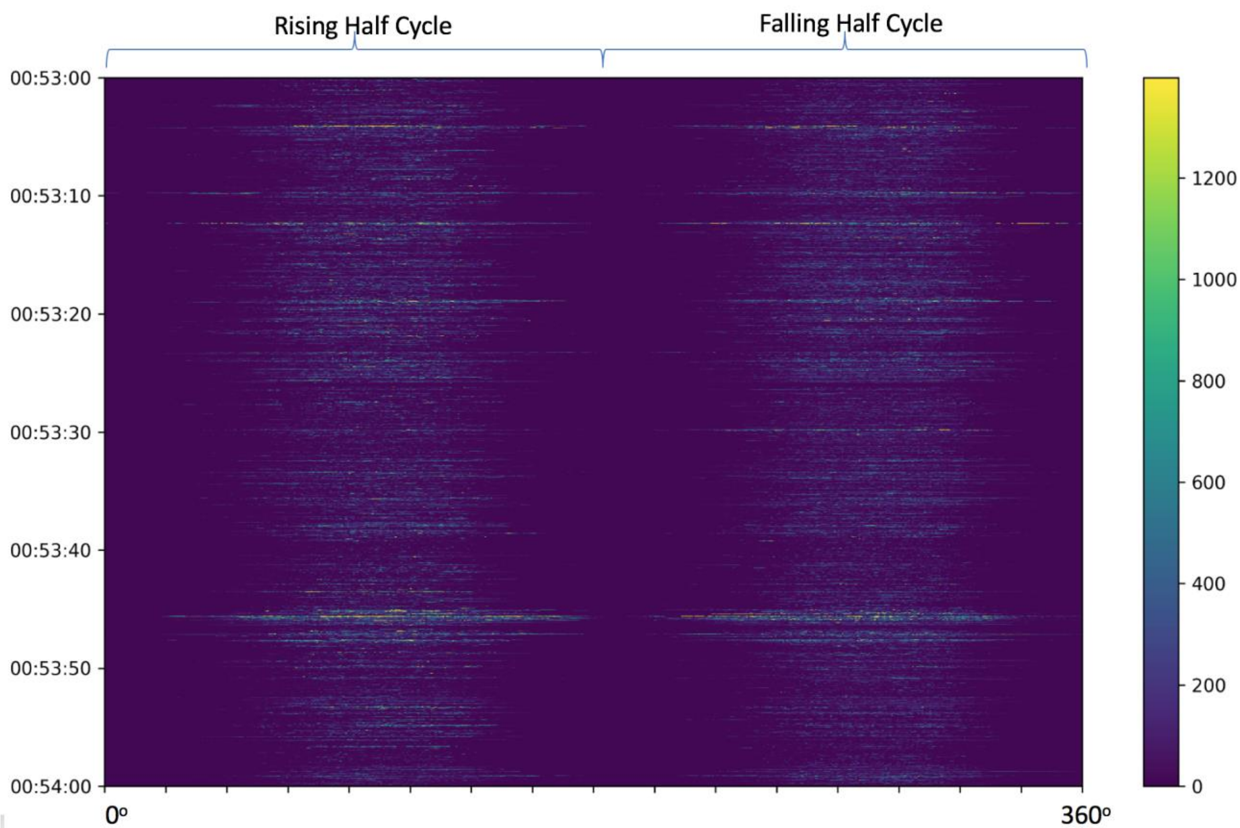

Figure 19 – Color Plot of fire pre-cursor signals over time. Colors denote the amplitude of the sensor signal detected.

For comparison, figure 21 shows the same color plot for a device running on the electrical network that is generating HF electrical activity. A typical feature of devices running on an electrical network is that HF electrical activity is in repeatable places in the phase over longer periods of time. This is indicated by the vertical lines in the falling half cycle. Ting algorithms exploit the differences between man-made devices which generate predictable and repeating signals from fire precursor signals which are more variable in time and amplitude.

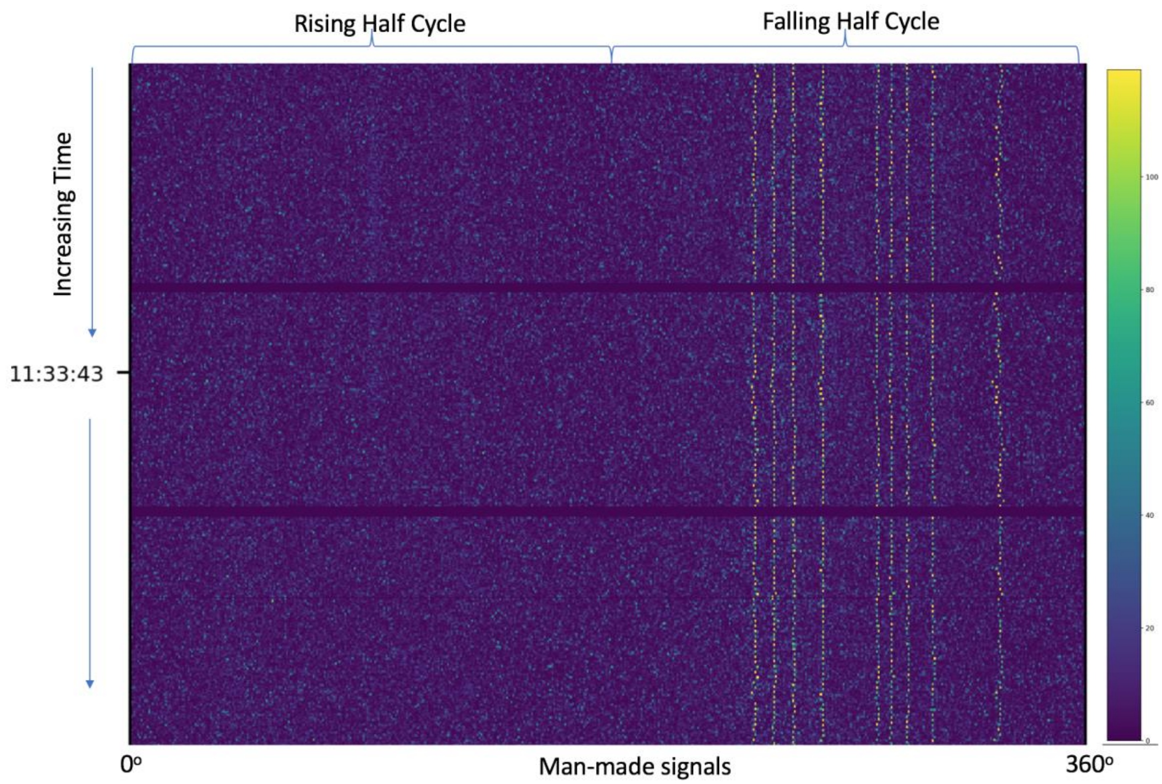

FIGURE 21 – COLOR PLOT OF A DEVICE WHICH CREATES RF NOISE IN A REPEATABLE PATTERN.

Figure 22 shows data from a single test home which is running a Ting sensor and a Proxy device on a separate circuit. The Ting sensor output which indicates a level of high frequency (HF) electrical activity is shown in blue. The HF electrical activity is shown in dimensionless units which indicates the strength of the HF electrical activity detected. Typical baseline output of the sensor is in the range of 2 to 50. When there are large amounts of electrical activity, this value can get as high as 4000. The output of the fire precursor detection algorithm is shown in red. The algorithm indicates a "1" when it detects fire precursor pulses and "0" when it does not. The HF electrical activity is just one of a set of features we use to determine if the electrical activity is caused by fire precursors. The amplitude and variability are one aspect, but as can be seen in figure 18, this is not the only aspect used in the algorithm. HF electrical activity at the start of the time period is generally at the same amplitude and variability as during the fire precursor detection period. The only HF electrical activity that triggers the Ting algorithms are signals generated by the proxy device. Because these signals are representative of those recorded in the lab of true fire precursors, this demonstrates the effectiveness of the Ting sensor and Ting algorithms to detect fire precursor signals and differentiate between fire precursor signals and those created by man-made devices connected to the electrical network.

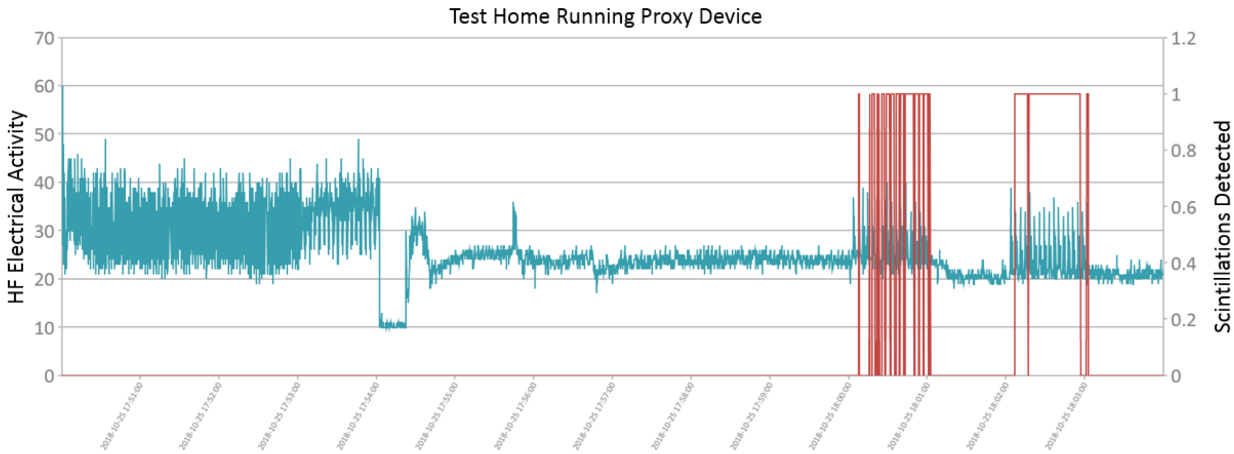

FIGURE 22 – OUTPUT FROM A SINGLE SENSOR DEVICE RUNNING IN A TEST HOME WITH THE PROXY DEVICE ON ANOTHER OUTLET. BLUE LINE INDICATES THE MAGNITUDE OF HF ELECTRICAL ACTIVITY OVER TIME. THE RED LINE SHOWS AN OUTPUT OF ONE WHEN TING ALGORITHMS CONSIDER THE HF ACTIVITY TO BE RELATED TO FIRE PRECURSOR SIGNALS, OTHERWISE THE OUTPUT IS ZERO.

In order to test the Ting Sensor and Proxy at multiple houses, we shipped Ting Sensor and Proxy devices to pilot participants. Participants installed the devices using a mobile application downloaded from the Google Play or Apple App stores. The mobile application instructs the participant how to install the devices and get them connected to Wi-Fi. They are instructed to install the sensor in less often or rarely used room in the house. They are instructed to install the Proxy device in any random outlet in the home provided it has adequate Wi-Fi signal. In this way, we get a random sampling of different power network endpoints to calculate detection efficiency within a sample of homes.

Detection Efficiency

The table below summarizes results from the pilot deployments described in the section above. For a detection to be counted, the sensor has to

1) Be able to detect the sensor on the electrical network. i.e. the signal is strong enough to be detected by the Ting sensor.
2) Present sufficient fire pre-cursor characteristics such that it is distinguishable from HF activity created by man-made devices on the electrical network.

Homes with Proxy Installed	# Homes Proxy Detected	# Homes Proxy Not Detected	Detection Efficiency
185	146	39	78.9%

FIGURE 23 – SUMMARY OF DETECTION EFFICIENCY OF PROXY DEVICE.

Detection of the proxy signal is a binary event: detection is successful or not. The estimated detection efficiency of the system is (approximately) the number of homes in which the proxy is detected divided by the total number of homes in which the test occurs. Any finite sample of homes will result in an imperfect estimate of the detection efficiency, and this is represented as a confidence interval.

The tests can be approximated by a binomial random variable. This modeling requires that it is reasonable to say that the detection probability is fixed across the population and trials in different homes are independent. This will be covered in the discussion.

A plot of the confidence interval vs number of homes is shown below. This assumes a single Proxy and Ting sensor location per home. The interval is the half-sided confidence interval (CI) where the full estimate is of the form $\hat{p} \pm CI$. The estimate of the binomial probability is close to the sample mean, and the CI is an estimate that in 95% of cases, the true detection efficiency lies within the stated interval.

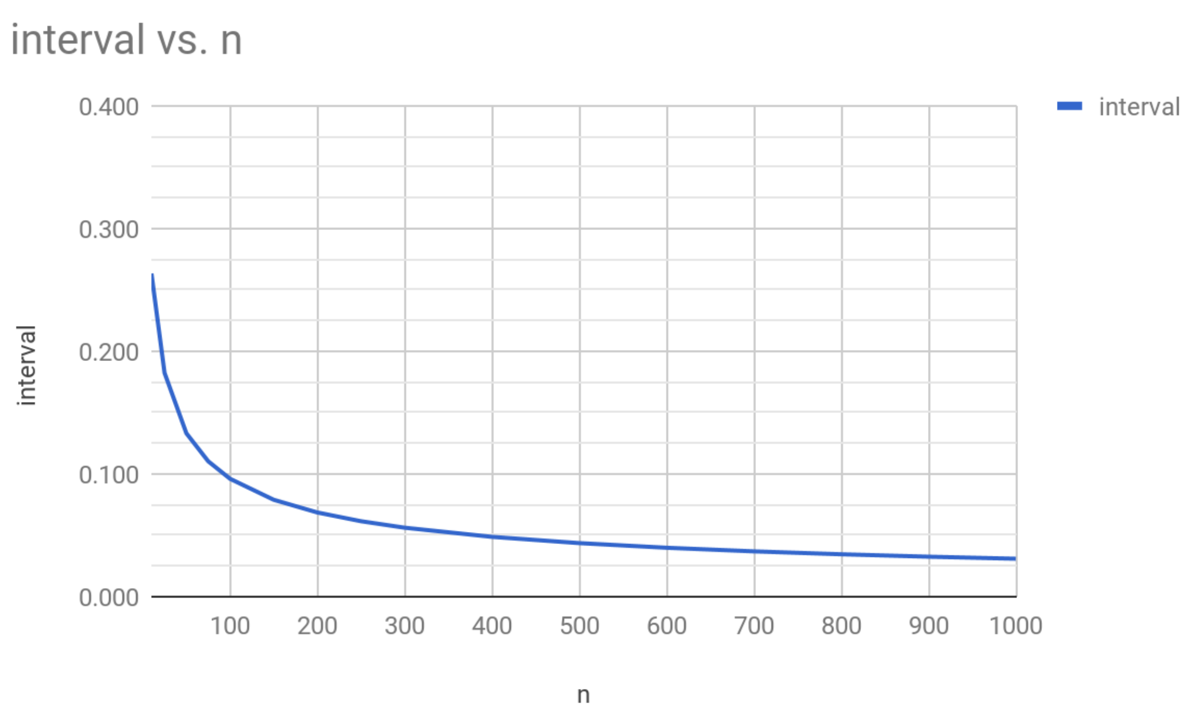

What this shows is that for relatively small sample sizes (e.g., n = 100), the confidence interval is less than ±10%. As the sample size grows, there is a diminishing return on the value of larger samples, and the improvement increases as the square root of the sample size. For example, a four times larger sample results in a confidence interval that is half as large. The difference between 1000 proxies and 4000 proxies is an interval of 3% and 1.5% respectively. Some key sample sizes are shown in the table below along with their worst-case sample confidence intervals (as the sample mean moves away from 50%, the confidence interval decreases).

Sample Size	CI
10	26%
25	18%
50	13%
100	10%
185	7%
250	6%
1000	3%

Impact of assumptions of independence and fixed detection probability

Few real-world situations are fully represented by the binomial distribution, and independence of the tests is often in question. In the case of the proxy testing, it is possible to develop a pilot that clearly violates the independence assumption. Tests conducted in homes in a single neighborhood where the homes are of a similar design, the same age, and the sensor and proxy are each plugged into nearly the same locations in each home will not be independent from one another.

By deploying to homes that are different in meaningful ways there is enough independence to ensure the assumption is valid. Age, size, and generalized layout are likely to be key differentiating factors. With relatively small samples of homes of different ages, sizes, and layouts, it is be possible to come up with good estimates for detection efficiency in homes between 1500 and 2500 square feet, for example, if there were 50 homes approximately uniformly distributed in that size range. Similar statements could be made on home age, or two story versus one story homes.

In this case, we have deployed the proxy to 185 homes which gives a confidence interval of about 7%.

False Alarm Rate

The Ting system is designed to algorithmically flag specific signals that have positive correlation with arcing activity. Flagged events are then sent to a team of experts for further review. There are several metrics that are reviewed by the expert team to determine whether or not a fire risk is present at the home. The vast majority of events are not fire hazards, and the relevant data is tagged for further machine learning improvement. When a fire hazard is identified, the Ting operations team notifies the homeowner, and a licensed electrician is deployed to the home to locate and mitigate the fire hazard.

False alarm rate (FAR) is best measured in false alarms per house-year where the target value is a rate far lower than one. Of the 200 Ting sensors deployed, (a value that includes homes with Ting sensors that did not receive a Proxy because these homes can also be subject to false alarm) there have only been two homes where the Ting system produced an alert that was confirmed by the expert team as a fire hazard. In the first case, an electrician visited the home and evidence of a fire hazard was found. In the second case, an electrician visited the home, however when the electrician arrived, the arcing stopped (Not a surprising outcome given the intermittent nature of arcing activity). The second home is still under observation by the Ting system for future arcing activity and thus the case has not yet been closed.

The calculation of FAR is a combination of:

1) Total number closed cases of homes where potential fires hazards were identified (I).

2) Total number of homes where evidence of a fire hazard was found (E).

This gives us an equation for false alarm rate as follows: $FAR = (I - E) / I$

Given that only 2 homes have been flagged for visits thus far, statistics are still too nascent to be of any value. The Whisker Labs team will continue monitoring and logging all detection events and will update this paper with conclusive statistics once they are available.

Summary

Electrical malfunctions are a leading cause of electrical fires which are estimated to cause 420 deaths, 1,370 injuries, and $1.4B in residential damages annually [3]. Electrical fires start when insulators fail to insulate, or conductors fail to conduct. The fire hazard starts when insulators or conductors first fail, and progress until sufficient heat is generated to ignite nearby materials. The process can take anywhere from hours, to weeks or years [11]. During this process, scintillations, or micro-arcs occur which produce small, rapidly changing currents. The micro-arcs have high frequency content that travels over the home’s electrical network, much like the signals commonly used for power line communications. Because these signals from scintillations travel throughout the home’s electrical network, a single device plugged into any outlet in the home is able to detect them. In this paper, we have demonstrated that the Ting device is able to detect scintillation-like signals produced by a simulator (proxy) device with a detection efficiency of 78.9% in 185 homes with a confidence interval of ~7%. Ting algorithms automatically flag electrical activity which correlate to arcing activity for a team of experts to quickly review and verify the presence of a fire risk. When a risk is identified, an operations team notifies the homeowner, and a licensed electrician is deployed to mitigate the hazard.

References

(1) https://www.usfa.fema.gov/data/statistics/

(2) https://www.usfa.fema.gov/downloads/pdf/statistics/v14i13.pdf

(3) https://www.nfpa.org/-/media/Files/News-and-Research/Fire-statistics/Major-Causes/osHomeElectricalFires.pdf

(4) https://plumblineservices.com/help-guides/how-much-does-an-afci-breaker-cost

(5) https://www.transparencymarketresearch.com/arc-fault-circuit-interrupter-market.html

(6) Benfer, Matthew E., and Gottuk, Daniel T., Development and Analysis of Electrical Receptacle Fires, Hughes Associates Technical Report, Project 1DTG00001.003, Sep. 2013.

(7) Billings, M. J., Smith, A., and Wilkins, R., Tracking in Polymeric Insulation, IEEE Trans. on Electrical Insulation IE-2, 131-137 (Dec. 1967).

(8) Groves, D. J., and Kaye, P. H., Tracking Events within a Dry Band, pp. 270-273 in 3rd Intl. Conf. on Dielectric Materials, Measurements and Applications (IEE Conf. Publ. 177), IEE, London (1979).

(9) Shea, J. J. (2011), Identifying causes for certain types of electrically initiated fires in residential circuits. Fire and Materials, 35: 19-42. doi:10.1002/fam.1033

(10) Shea, J. J. (2006) "Glowing Contact Physics," Electrical Contacts - 2006. Proceedings of the 52nd IEEE Holm Conference on Electrical Contacts, Montreal, QC, 2006, pp. 48-57.

(11) Twibell, J. D., Electricity and Fire, pp. 61-104 in Fire Investigation, N. N. Daéid, ed., CRC Press, Boca Raton FL (2004).

(12) Yereance, R. A., and Kerkhoff, T., Electrical Fire Analysis, 3rd ed., Page 206, Charles C. Thomas, Springfield IL (2010).

(13) http://www.isplc.org/docsearch/Proceedings/1999/pdf/0566_001.pdf

(14) C. Thoradson, 'Meters', US Patent Nos. 784712 and 784713, 1905

(15) "IEEE Standard for Broadband Over Power Line Networks: Medium Access Control and Physical Layer Specifications, IEEE Standard 1901-2010", Sep. 2010.

(16) https://www.netgear.com/home/products/networking/powerline/default.aspx

(17) C. Cano, A. Pittolo, D. Malone, L. Lampe, A. M. Tonello, A. G. Dabak, "State of the art in power line communications: From the applications to the medium", IEEE J. Sel. Areas Commun., vol. 34, pp. 1935-1952, Jul. 2016.
https://arxiv.org/pdf/1602.09019.pdf

(18) M. Tlich, A. Zeddam, F. Moulin, F. Gauthier, "Indoor power-line communications channel characterization up to 100 MHz—Part I: One-parameter deterministic model", IEEE Trans. Power Del., vol. 23, no. 3, pp. 1392-1401, Jul. 2008.

(19) INTERNATIONAL JOURNAL OF COMMUNICATION SYSTEMS
Int. J. Commun. Syst. 2003; 16:381–400 (DOI: 10.1002/dac.596)
In-building power lines as high-speed communication channels: channel characterization and a test channel ensemble
Tooraj Esmailian,, Frank R. Kschischang2 and P. Glenn Gulak

(20) E. Liu, Y. Gao, O. Bilal, and T. Korhonen, “Broadband characterization of indoor powerline channel,” in Proc. Int. Symp. Power Line Commun., Zaragoza, Spain, 31 Mar.–2 Apr. 2004

(21) V. Babrauskas, “Mechanisms and modes for ignition of low-voltage,PVC-insulated electrotechnical products”, Fire Mater. 2006; 30:151–174

(22) X. Zhou, J. Shea, and B. Pahl, “Characterization of EMI/RFI in Commercial and Industrial Electrical Systems”, 2013 IEEE 59th Holm Conference on Electrical Contacts

(23) Q. Zibo, G. Wei, and G. Chen, “The Development of AC Arc Fault Simulation Test Device with Arc Breaking Function”, 2017 IEEE International Conference on Computational Science and Engineering

(24) V. Babrauskas, “Fires originating in branch-circuit NM cables due to installation damage”, Journal of Fire Sciences 2018, Vol. 36(5) 438-450

(25) G. Artale, A Cataliotti, et al, “Experimental characterization of series arc faults in AC and DC electrical circuits”, 2014 IEEE International Instrumentation and Measurement Technology Conference Proceedings

(26) J. Wafer, “The Evolution of Arc Fault Circuit Interruption”, The 51st IEEE HOLM conference on Electrical Contacts, 2005.

Author Biographies

Dr. Heckman holds degrees in physics and atmospheric science. He is the scientist behind the successful development of the Earth Networks global lightning detection system. Stan currently leads the science efforts at Whisker Labs for the Ting sensor.

Mr. Sloop holds a degree in physics and computer engineering. He was a co-founder of Earth Networks (EN) and led development of many EN products over the years. He is currently leading development and engineering efforts for the Ting Sensor at Whisker Labs.

Dr. Babrauskas holds degrees in physics, structural engineering, and fire protection engineering. During the last two decades, he has done extensive research on physical mechanisms leading to electrical fires. He is currently preparing a monograph on electrical fires and explosions.

Dr. Hoppmann holds degrees in physics and bioengineering. He is the leading data scientist at Whisker Labs developing algorithms for detection of fire precursors with the Ting sensor.

Mr. Schetrit holds degrees in engineering and business. He is co-founder of Whisker Labs and is currently leading product development of the Ting sensor.